

A New Look at the YY CrB Binary System

SOMAYEH SOOMANDAR¹ AND ATILA PORO²

¹*Independent astrophysics researcher, Kerman, Iran*

²*Astronomy Department of the Raderon Lab., BC., Burnaby, Canada*

ABSTRACT

This study presented a new analysis for the TESS-observed W Ursae Majoris (W UMa) binary star YY Coronae Borealis (YY CrB). The light curve was analyzed by the PHysics Of Eclipsing BinariEs (PHOEBE) Python version together with the Markov chain Monte Carlo (MCMC) method. The light curve solutions required a hot spot and l_3 . New eclipse times from the TESS observations were extracted, and the O-C curve of primary and secondary minima showed an anti-correlated manner. In order to study the O-C curve of minima, minima times between 1991 and 2023 were collected. This investigation reported a new linear ephemeris and by fitting a quadratic function to the O-C curve of minima, calculated the orbital period rate of $\dot{P} \approx 5.786 \times 10^{-8} \frac{\text{day}}{\text{year}}$. Assuming mass conservation, a mass exchange rate of $M_2 = 2.472 \times 10^{-8}$ calculated from the more massive component to the less massive one. Then, by using the light travel time function, the possible third body was determined in the binary and derived the mass of the third body as $0.498 M_{\odot}$ with a period of $\simeq 7351.018$ days. The O-C curve analysis and the quantity of mass indicate that the presence of a third body is unlikely. This binary is expected to evolve into a broken-contact phase and is a good case to support the thermal relaxation oscillation model.

Keywords: binaries: eclipsing – method: photometric

1. INTRODUCTION

W UMa-type systems are recognised by their eclipsing light curves with almost equal minima and a short orbital period. These stars have spectral types ranging from A to middle K, and the convective atmosphere is the main reason for chromosphere activity, as well as starspots, which are signs of the existence of dynamo-generated magnetic activity.

YY CrB (HIP 77598, TIC 29287800) is a W UMa binary system discovered by Hipparcos [ESA 1997](#). This system has been studied in some works; first [Rucinski, et al. \(2000\)](#) revealed the spectral type F8V for two components. [Vařík et al. \(2004\)](#) found the light curves to be asymmetric and mentioned the existence of starspots on the components. [Gazeas et al. \(2005\)](#) analyzed the light curve and derived the geometric and photometric parameters and concluded that this target is a contact binary with weak magnetic activity.

[Essam et al. \(2010\)](#) combined photometric and spectroscopic solutions and calculated the fill-out factor approximately equal to 64 percent and mass ratio of 0.241. In addition, they studied the changes in the orbital period using the O-C diagram and concluded that the orbital period is decreasing. [Yu, Xiang, & Xiao \(2015\)](#) studied the orbital period changes and implied that the decreased period rate and concluded that the sinusoidal oscillatory can be interrupted as magnetic activity. [Essam et al. \(2010\)](#) and [Yu, Xiang, & Xiao \(2015\)](#) on the rate of period decrease demonstrate that the value of reduced rate is lowering progressively, indicating that this system was going through an orbital expansion stage of thermal relaxation oscillation (TRO) cycles. Also, understanding the evolutionary status of this target could prove invaluable. Using new space-based data, we have re-analyzed the light curve solution and studied the O-C curve in detail. Moreover, we studied the possibility of a third body in this interesting system. The structure of the paper is as follows: Section 2 provides information on TESS observations and a data reduction process. The light curve

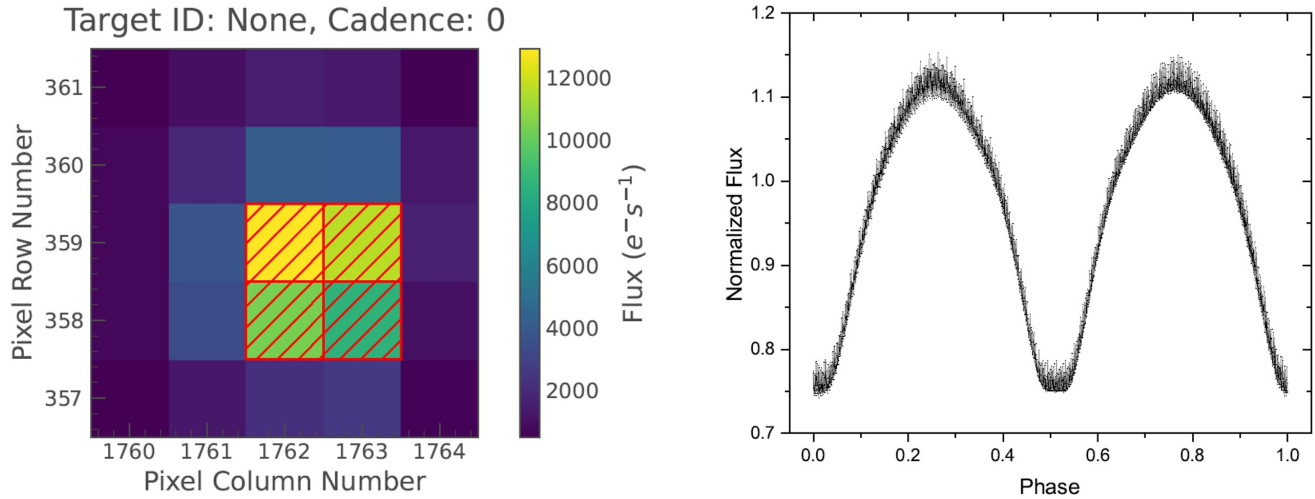


Figure 1. Left panel: TESS target pixel file of YY CrB in sector 51. The pixels included in the computation of the SAP as red bordered pixels. Right panel: phased light curve during sector 51.

solution and the estimation of absolute parameters are included in Sections 3 and 4 respectively, the orbital period variation analysis is presented in Section 5, and finally, Section 6 contains the discussion and conclusion.

2. OBSERVATION AND DATA REDUCTION

YY CrB was observed by the TESS during sectors 24 and 51 (April 16, 2020-May 13, 2020, and April 22, 2022-May 18, 2022) on Cameras 1 and 3. There is two-minute cadence data for sector 24 that are processed by the Science Processing Operations Center (SPOC) pipeline (Jenkins et al. (2016); Jenkins (2015)). Photometric photos were downloaded using the Lightkurve package (Lightkurve Collaboration et al. 2018) that provides the functions to download TESS data from the public data archive at MAST¹. For sector 24, we used the Pre-search Data Conditioning flux of the Simple Aperture Photometry (PDCSAP). There is no detrended light curve for sector 51. Therefore, we download the TESS Full Frame Images (FFIs) from the MAST and used Lightkurve package to extract the SAP light curve with a mask that are defined by the pixels shown in the left panel of Figure 1. We used `create_threshold_mask` function to produce an aperture mask using a threshold equal to 10. This function identifies the pixels in the target pixel file and shows that a median flux that is brighter than the threshold times the standard deviation above the overall median. The right panel of Figure 1 shows the phased light curve that was produced.

3. LIGHT CURVE SOLUTION

Essam et al. (2010) calculated the optimal parameters by combining simultaneous radial velocity and light curve solutions. We started with the initial values of the parameters taken from the solution by the Essam et al. (2010) study. One-day data from TESS sector 24 were utilized to light curve solution. The observation of 2-min cadence help to better analysis of the effect of spots on the components. Photometric analysis of the YY CrB system was carried out using the PHOEBE 2.4.9 version, TESS filter of the code, and the MCMC approach (Prša & Zwitter 2005, Prša et al. 2016, Conroy et al. 2020, Poro et al. 2022).

We selected the TESS passband from the code and chose the contact binary mode in the PHOEBE based on the light curve's shape and solutions of previous studies.

¹ <https://mast.stsci.edu>

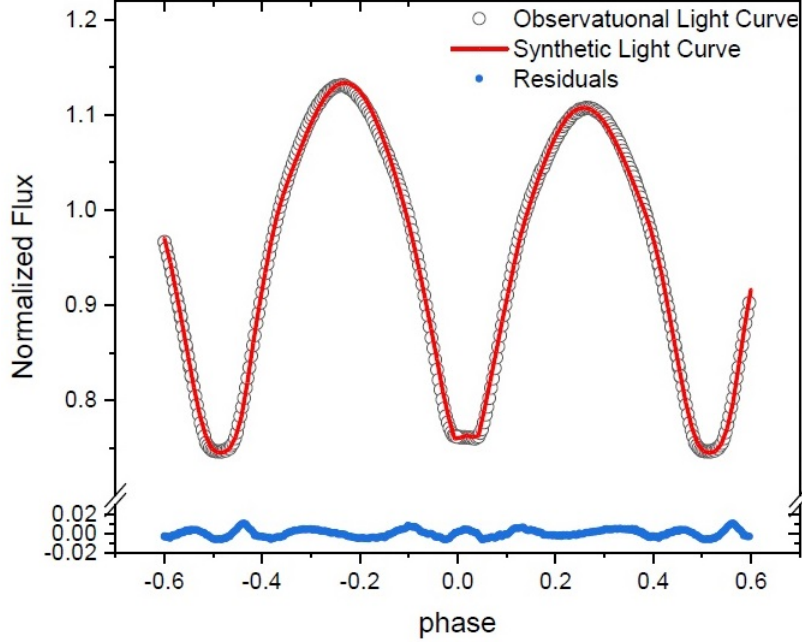


Figure 2. Light curve solution of the eclipsing binary YY CrB. Observational light curve (blank circle), synthetic light curve (solid red line), and the residuals (blue circle).

The initial and input parameters were as follows: The mass ratio $q = 0.241$ and the effective temperature of primary component $T_1 = 5819$ are (Essam et al. 2010), the gravity darkening coefficients, $g_1 = g_2 = 0.32$ and the albedo coefficients, $A_1 = A_2 = 0.5$ (Lucy 1967, Ruciński 1969).

The limb-darkening coefficients were employed as free parameters, and the Castelli & Kurucz (2004) method was used to model the stellar atmosphere. The parameters searched in MCMC include: the orbital inclination i , the mean temperature of the stars $T_{1,2}$, the mass ratio q , the fillout factor f , the bandpass luminosity of the primary star (L_1), and the third light in total light (l_3). We applied 46 walkers and 1000 iterations to each walker in MCMC. According to the asymmetry in the brightness of maxima in the light curve of the close eclipsing binary, the solution requires the assumption of a hot spot on the primary component (O'Connell 1951). According to observational and theoretical light curves in this study, it has not been possible to provide the solution without considering l_3 . The theoretical fit on the observational light curve for the YY CrB system is given in Figure 2. The corner plot that MCMC produced is displayed in Figure 3. Also, the geometrical structure is plotted in Figure 4, which has a lower temperature at the point of contact between companion stars due to the gravity darkening (Prša et al. 2016). The calculated parameters together with the values obtained by Essam et al. (2010) are listed in Table 1.

4. ABSOLUTE PARAMETERS

The absolute parameters of the binary system including $M_{v1,2}$, $M_{bol1,2}$, $L_{1,2}$, $R_{1,2}$, $M_{1,2}$, $\log(g)_{1,2}$, and a were calculated. We used Gaia DR3 parallaxes and the parameters of the light curve solution in this study. We followed the same method as done by Poro et al. (2022). First the absolute magnitude M_v of the system was calculated by Equation (1).

$$M_{v(system)} = V_{max} - 5 \log(d) + 5 - A_v \quad (1)$$

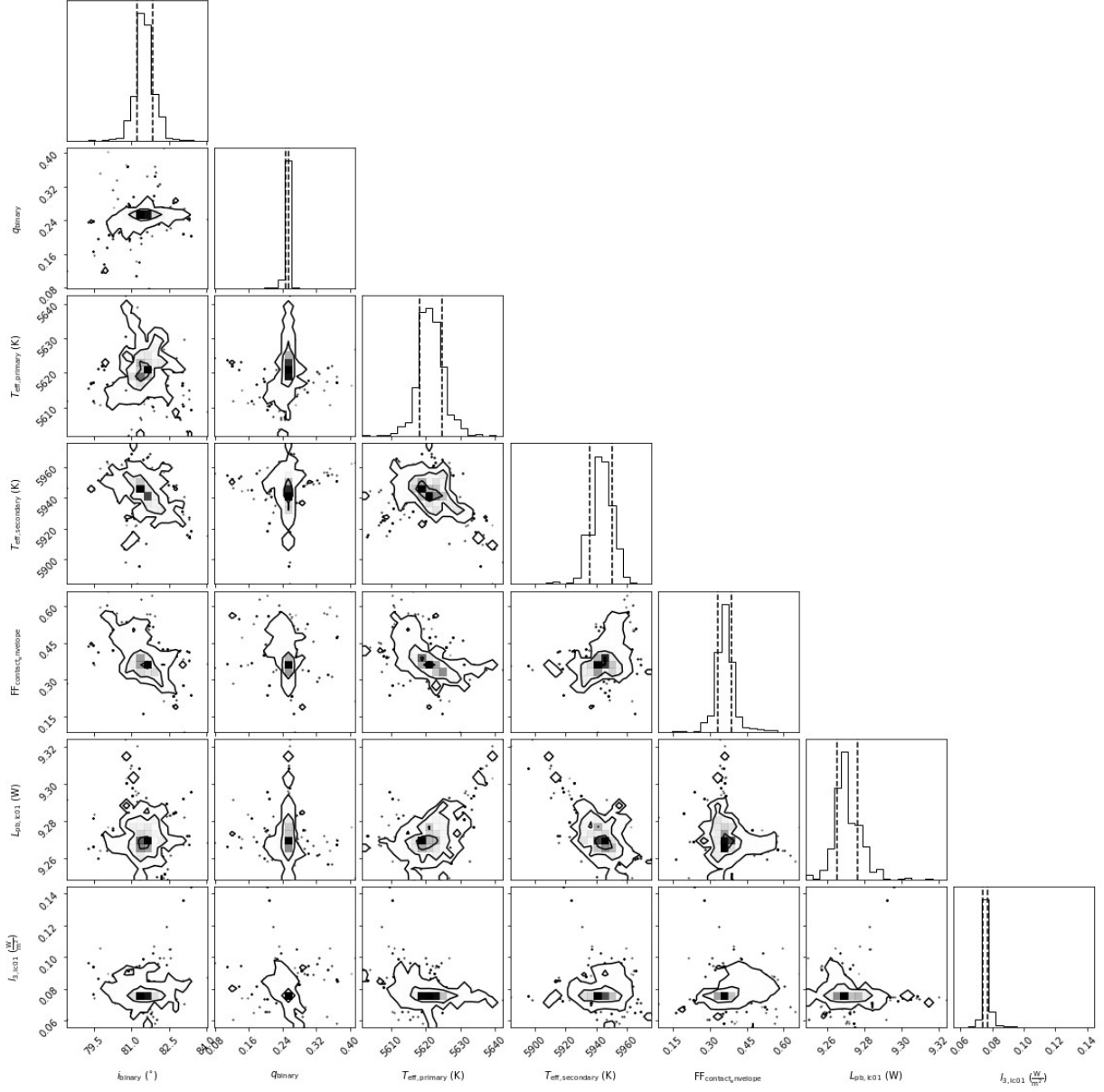


Figure 3. The corner plots of the light curve solution.

where the distance of the system from Gaia DR3 ($d_{pc} = 90.07 \pm 0.1$) was derived and $V_{max} = 8.64 \pm 0.08$ comes from the VSX² database. Extinction coefficient $A_v = 0.015 \pm 0.002$ was obtained using the DUST-MAPS package in Python (Green et al. 2019). Also, Equation (2) can be utilized to determine the primary and secondary components' absolute magnitude.

$$M_{v1,2} - M_{vtot} = -2.5 \log\left(\frac{l_{1,2}}{l_{tot}}\right) \quad (2)$$

The bolometric magnitude M_{bol} of each component of the binary was obtained by Equation (3),

² <https://www.aavso.org/vsx/>

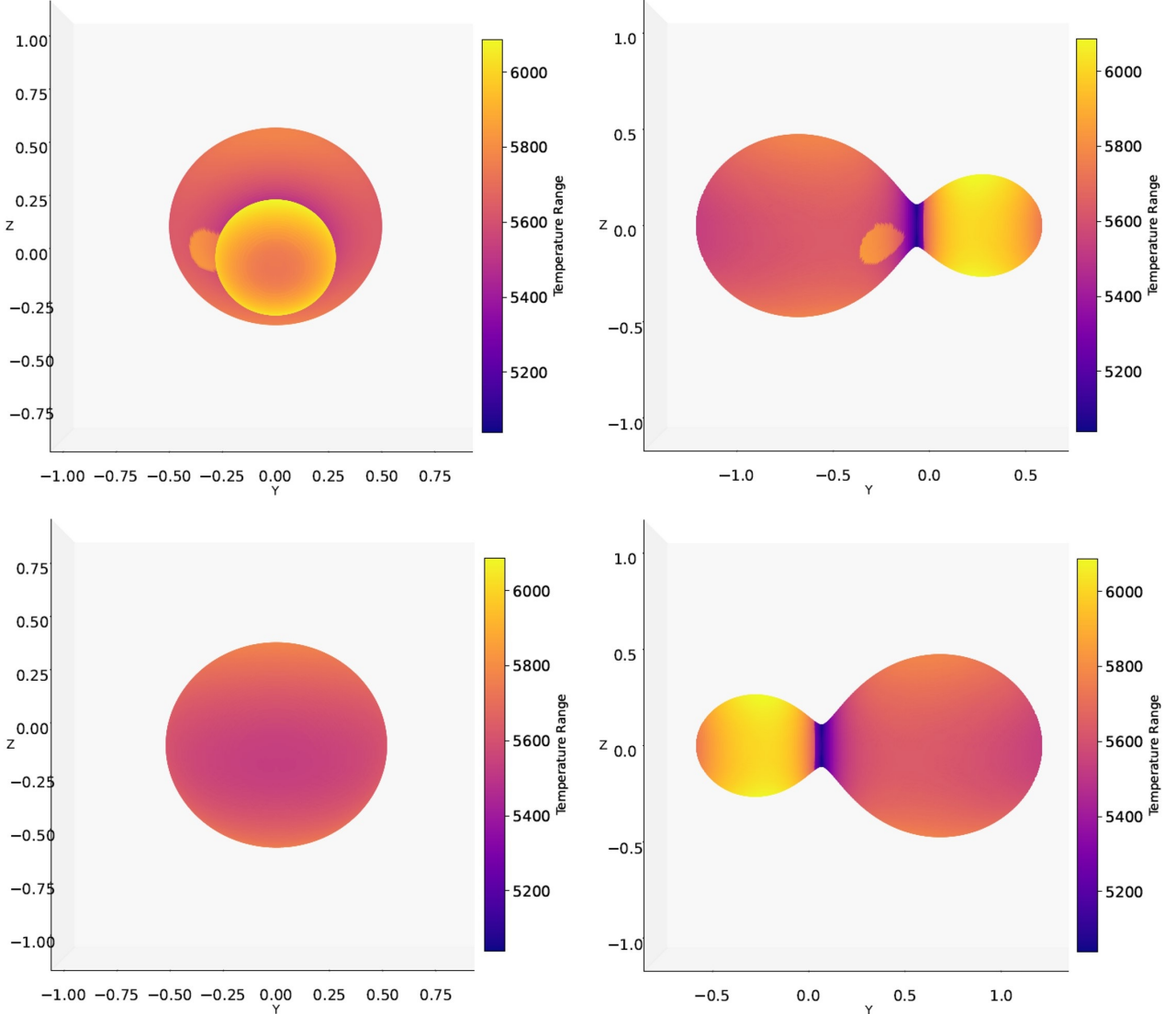


Figure 4. The geometrical structure of YY CrB.

$$M_{bol} = M_v + BC \quad (3)$$

where the effective temperature of the stars is employed to obtain the bolometric correction for the primary and secondary components retrieved $BC_1 = -0.111$ and $BC_2 = -0.052$ respectively (Flower 1996). The bolometric correction is presented as polynomial fits in Equation (4).

$$BC = a + b(\log T_{eff}) + c(\log T_{eff})^2 + d(\log T_{eff})^3 + e(\log T_{eff})^4 \quad (4)$$

Then, the luminosity of two components is determined from Pogson's relation (Pogson 1856),

$$M_{bol} - M_{bol\odot} = -2.5 \log\left(\frac{L}{L_\odot}\right) \quad (5)$$

where $M_{bol\odot}$ is taken as 4.73^{mag} from Torres (2010). The radius of primary and secondary components is calculated by the equation (6),

$$R = \left(\frac{L}{4\pi\sigma T^4}\right)^{1/2} \quad (6)$$

Table 1. The parameters of the eclipsing binary YY CrB.

Parameter	This study	Essam et al. (2010)
$q = M_2/M_1$	$0.2498^{+0.0031}_{-0.0024}$	0.241 ± 0.002
T_1 (K)	5621^{+3}_{-3}	5819
T_2 (K)	5944^{+6}_{-8}	6010 ± 72
i (deg)	$81.50^{+0.36}_{-0.29}$	80.26 ± 0.05
$\Omega_1 = \Omega_2$	2.295 ± 0.079	2.237
l_1/l_{tot}	$0.730^{+0.001}_{-0.001}$	0.7508 ± 0.0154
l_2/l_{tot}	0.264 ± 0.001	0.2492
l_3/l_{tot}	$0.006^{+0.001}_{-0.001}$	
f	$0.363^{+0.025}_{-0.031}$	0.64
r_{1mean}	0.522 ± 0.018	0.537
r_{2mean}	0.287 ± 0.028	0.282
Phase shift	0.08 ± 0.005	
Spot on the star 1:		
Colatitude θ	99 ± 1	90
Longitude λ	325 ± 1	11.25 ± 1.638
Angular radii γ	18 ± 1	5.250 ± 0.573
T_{star}/T_{spot}	1.04 ± 0.02	0.750
Spot on the star 2:		
Colatitude θ		99.487 ± 3.919
Longitude λ		325
Angular radii γ		16.300 ± 1.326
T_{star}/T_{spot}		1.351

where the σ is the Stephen-Boltzmann constant and T is the temperatures of each components.

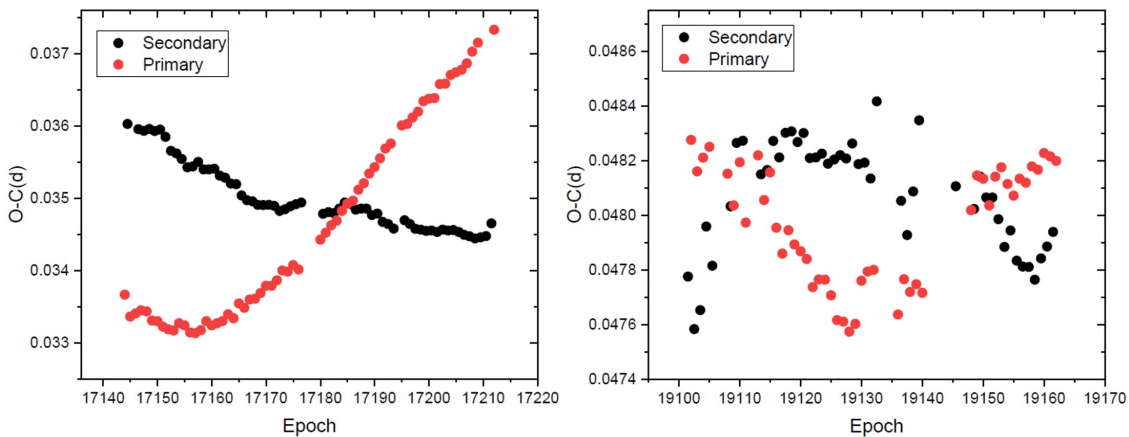
Additionally, with considering $r_{mean1,2}$ and $a = \frac{R}{r_{mean}}$, we calculated the separation a in average a_1 and a_2 . The resulting parameters and the values obtained by the Essam et al. (2010) study are listed in Table 2.

5. THE ORBITAL PERIOD CHANGES

To calculate the eclipse times of minima, we used the same method as done by Soomandar & Abedi (2020). First, split the detrended light curves for individual eclipses and fit a Lorentzian function to each eclipse by using the least-squares method. We used the `Scipy.curve-fit` package in Python to fit the Lorentzian function to the individual eclipses. We used the `np.sqrt(np.diag(cov))` function to calculate the standard deviation errors on the parameters. TESS

Table 2. The absolute parameters of YY CrB.

Absolute parameters	This study	Essam et al. (2010)
$M_{bol1}(mag)$	4.083 ± 0.074	3.939
$M_{bol2}(mag)$	5.246 ± 0.072	5.173
$L_1(L_\odot)$	1.832 ± 0.121	2.580
$L_2(L_\odot)$	0.628 ± 0.041	0.668
$R_1(R_\odot)$	1.430 ± 0.049	1.427
$R_2(R_\odot)$	0.749 ± 0.026	0.757
$a(R_\odot)$	2.674 ± 0.080	2.64
$M_1(M_\odot)$	1.448 ± 0.131	1.467
$M_2(M_\odot)$	0.362 ± 0.037	0.357
$\log(g)_1(cgs)$	4.288 ± 0.008	4.295
$\log(g)_2(cgs)$	4.248 ± 0.012	4.232

**Figure 5.** Left panel: primary and secondary O-C curve of minima for sector 24. Right panel: primary and secondary minima for sector 51 (primary O-C curve in black circles and secondary O-C curve in red circles.).

observations yielded a total of 220 primary and secondary minima, as displayed in the table 3. The new observational eclipse times were calculated. Then, we performed an analysis of observed (O) minus calculated (C) eclipse times (Sterken 2005). We calculated the O-C curve using the following linear ephemeris (Kreiner 2004, Yu, Xiang, & Xiao 2015):

$$\text{Min.I} = 2452500.1757 + 0.3765545 \times E \quad (7)$$

The O-C curve of primary and secondary minima for sectors 24 and 51 are plotted in Figure 5. The anti-correlated manner between primary and secondary minima is obvious which is a confirmation of the presence of spots on the contact binary components (Tran et al. (2013); Balaji et al. (2015)). We averaged primary and secondary minima to eliminate the anti-correlated impact when analyzing orbital period changes (Balaji et al. 2015). The calculated values are shown in Table 3. 109 YY CrB observational minima times were recorded in the literature over a 31-year period. The appendix contains a list of the data gathered with uncertainty. Observational minima times converted to BJD-TDB³. Figure 6's left panel depicts the O-C curve of the minima. We presented a new ephemeris for this target as Equation (8) by fitting a linear function on the O-C curve of primary.

$$\text{Min.I} = 2458955.8598(\pm 1.1e - 4) + 0.3765581(\pm 1.1e - 7) \times E \quad (8)$$

³ <https://astroutils.astronomy.osu.edu/time/hjd2bjd.html>

The O-C curve of minima is calculated with the new ephemeris and the resulting curve shows the same shape as the left panel of Figure 6. we fitted a quadratic function to the O-C curve in order to investigate the variations in the orbital period:

$$T_{mid}(E) = T_0 + PE + \frac{1}{2} \frac{dP}{dt} E^2 \quad (9)$$

where mid-eclipse times T_{mid} are described by T_0 is the reference mid-eclipse time, P is the orbital period and, E is the epoch of eclipses (Patra et al. 2017). And the quadratic fit showed a drop in period, which corresponded to the quadratic plot in Figure 6's left panel. We determined the rate of period decline using the model's quadratic coefficient as Equation (10)

$$\dot{P} = \frac{2 \times -1.124 \times 10^{-11}}{0.3765545} = -5.786 \times 10^{-8} \pm 9.965 \times 10^{-9} \frac{\text{day}}{\text{year}} \quad (10)$$

Considering $M_1 = 1.448M_\odot$ for the primary and $M_2 = 0.362M_\odot$ for the secondary one calculated in this study and using Equation (11) and mass conservation, the rate of mass exchange between primary and secondary components was estimated.

$$\frac{\dot{P}}{P} = -3 \frac{\dot{M}_2(M_1 - M_2)}{M_1 M_2} \Rightarrow \dot{M}_2 = +2.472 \times 10^{-8} \pm 0.190 \times 10^{-8} M_\odot \text{yr}^{-1} \quad (11)$$

The positive sign indicates the direction of mass transfer from the more massive to the less massive component. The cyclic changes are shown by the residuals of the quadratic fit. As a result, we investigated the Light Travel Time Effect (LTTE) as a possible cause of the O-C curve variations. The following periodogram analysis was performed with the Period 04 software (Lenz & Breger 2005) for the residuals of a quadratic fit. The peak of frequencies in the periodogram analysis of residuals shows a period of 7351.018 days. Then, we used the least square method to fit the Light Travel Time (LTT) formula on the O-C curve (Irwin 1952):

$$(O - C)_{LTT} = A \times \left(\frac{1 - e^2}{1 + e \cos v} \sin(v + \omega) + e \sin(\omega) \right) \quad (12)$$

where $A = \frac{a_{12} \sin i}{c}$, and a_{12} is the semi-major axis of the relative orbit of the eclipsing system around the center of mass (in Au unit), i is the inclination of the third-body orbit, e is the eccentricity of the supposed third body, ω is the longitude of periastron passage in the plane of the orbit and, v is the true anomaly. To fit the LTT function to the residuals of the O-C curve, we have to convert the epoch to the true anomaly and Kepler's formula provides the link between the eccentric anomaly and the observed eclipse time:

$$E_3 - e \sin E_3 = \frac{2\pi}{P_3} (t - T_0) \quad (13)$$

The equation (13) was calculated using Newton-Raphson's method for every eclipse time of minima and considering equation (14) the epochs converted to the true anomaly.

$$\begin{aligned} \tan \frac{v}{2} &= (\frac{1+e}{1-e})^{1/2} \tan \frac{E_3}{2} \\ t &= T_0 + \text{epoch} \times P_{binary} \end{aligned} \quad (14)$$

where P_{binary} , t , P_3 , E_3 , and T_0 are the period of binary, the time of observed minima, the period of the third body, the eccentric anomaly and, the time of periastron passage respectively. By assuming a coplanar orbit ($i = 90$), we determined the lower limit for the mass of the third body. The calculated parameters of the third body are listed in Table 5 and the related curve is plotted in the right panel of Figure 6.

Assuming the third body is a main-sequence star, this corresponds to the M1V spectral type with a brightness of $0.041L_\odot$ ⁴, or 0.016 of the total luminosity which doesn't agree with the value l_3 determined in section 3.

We are not certain that l_3 produced from the TESS light curve analysis represents a valid observation of flux from a third body in the system, despite the computation of the effect of the third body, especially as there is no exact

⁴ http://www.pas.rochester.edu/~emamajek/EEM_dwarf_UBVIJHK_colors_Teff.txt

Table 3. Extracted the times of minima from TESS observations. All times of minima have been reduced to 2450000. Additionally, the minimum error is equal to 0.0001.

Min.	Epoch	O-C									
8955.8597	17144	0.0337	8966.5927	17172.5	0.0348	8978.8326	17205	0.0368	9702.0170	19125.5	0.0482
8956.0504	17144.5	0.0360	8966.7802	17173	0.0340	8979.0187	17205.5	0.0345	9702.2047	19126	0.0351
8956.2360	17145	0.0336	8966.9693	17173.5	0.0348	8979.2092	17206	0.0368	9702.2047	19126	0.0476
8956.6126	17146	0.0334	8967.1567	17174	0.0340	8979.3952	17206.5	0.0344	9702.3936	19126.5	0.0482
8956.8034	17146.5	0.0359	8967.3459	17174.5	0.0349	8979.5859	17207	0.0369	9702.5813	19127	0.0476
8956.9892	17147	0.0334	8967.5334	17175	0.0341	8979.7718	17207.5	0.0345	9702.7702	19127.5	0.0482
8957.1799	17147.5	0.0359	8967.7225	17175.5	0.0349	8979.9626	17208	0.0370	9702.9578	19128	0.0475
8957.3657	17151	0.0002	8967.9099	17176	0.0340	8980.1483	17208.5	0.0344	9703.1468	19128.5	0.0482
8957.3657	17148	0.0334	8968.0990	17176.5	0.0349	8980.3392	17209	0.0371	9703.3343	19129	0.0476
8957.5565	17148.5	0.0359	8969.4165	17180	0.0344	8980.5249	17209.5	0.0344	9703.5233	19129.5	0.0482
8957.7421	17149	0.0333	8969.6050	17180.5	0.0348	8980.9014	17210.5	0.0345	9703.7111	19130	0.0477
8957.9331	17149.5	0.0359	8969.7931	17181	0.0345	8981.2781	17211.5	0.0346	9703.8998	19130.5	0.0482
8958.1187	17150	0.0333	8969.9817	17181.5	0.0348	8981.4691	17212	0.0373	9704.0876	19131	0.0478
8958.3096	17150.5	0.0359	8970.1697	17182	0.0346	9692.9793	19101.5	0.0478	9704.2763	19131.5	0.0481
8958.4952	17151	0.0332	8970.3582	17182.5	0.0348	9693.1681	19102	0.0482	9704.4642	19132	0.0478
8958.6861	17151.5	0.0358	8970.5464	17183	0.0347	9693.3556	19102.5	0.0475	9704.6531	19132.5	0.0484
8958.8717	17152	0.0332	8970.7348	17183.5	0.0348	9693.5445	19103	0.0481	9705.9703	19136	0.0476
8959.0624	17152.5	0.0356	8970.9231	17184	0.0348	9693.7323	19103.5	0.0476	9706.1590	19136.5	0.048
8959.2482	17153	0.0332	8971.1114	17184.5	0.0349	9693.9211	19104	0.0482	9706.3469	19137	0.0478
8959.4390	17153.5	0.0356	8971.2997	17185	0.0349	9694.1092	19104.5	0.0479	9706.5354	19137.5	0.0479
8959.6249	17154	0.0333	8971.4880	17185.5	0.0349	9694.2977	19105	0.0482	9706.7234	19138	0.0477
8959.8155	17154.5	0.0355	8971.6763	17186	0.0349	9694.4855	19105.5	0.0478	9706.9121	19138.5	0.0481
8960.0014	17155	0.0332	8971.8645	17186.5	0.0348	9695.2398	19107.5	0.0489	9707.1000	19139	0.0477
8960.1919	17155.5	0.0354	8972.0531	17187	0.0351	9695.4272	19108	0.0481	9707.2889	19139.5	0.0483
8960.3778	17156	0.0331	8972.2411	17187.5	0.0348	9695.6154	19108.5	0.048	9707.4766	19140	0.0477
8960.5685	17156.5	0.0354	8972.4297	17188	0.0352	9695.8037	19109	0.0480	9708.2306	19142	0.0486
8960.7544	17157	0.0331	8972.6176	17188.5	0.0348	9695.9922	19109.5	0.0483	9709.5480	19145.5	0.0481
8960.9450	17157.5	0.0355	8972.8063	17189	0.0353	9696.1804	19110	0.0482	9710.4893	19148	0.048
8961.1310	17158	0.0331	8972.9941	17189.5	0.0348	9696.3688	19110.5	0.0483	9710.6776	19148.5	0.0480
8961.3215	17158.5	0.0354	8973.1830	17190	0.0354	9696.5567	19111	0.0479	9710.8660	19149	0.0481
8961.5077	17159	0.0333	8973.3707	17190.5	0.0348	9697.3101	19113	0.0482	9711.0543	19149.5	0.0481
8961.6980	17159.5	0.0354	8973.5597	17191	0.0355	9697.4983	19113.5	0.0481	9711.2425	19150	0.0481
8961.8842	17160	0.0332	8973.7471	17191.5	0.0347	9697.6865	19114	0.0480	9711.4307	19150.5	0.0481
8962.0746	17160.5	0.0354	8973.9364	17192	0.0357	9697.8749	19114.5	0.0482	9711.6190	19151	0.048
8962.2608	17161	0.0331	8974.1236	17192.5	0.0346	9697.8749	19114.5	0.0482	9711.8073	19151.5	0.0481
8962.4511	17161.5	0.0353	8974.3130	17193	0.0375	9698.0631	19115	0.0481	9711.9956	19152	0.0481
8962.6374	17162	0.0333	8974.5001	17193.5	0.0345	9698.2516	19115.5	0.0483	9712.1838	19152.5	0.048
8962.8276	17162.5	0.0353	8975.0664	17195	0.0360	9698.4395	19116	0.0479	9712.3722	19153	0.0482
8963.0140	17163	0.0334	8975.2533	17195.5	0.0347	9698.6281	19116.5	0.0482	9712.5602	19153.5	0.0479
8963.2041	17163.5	0.0352	8975.4430	17196	0.0360	9698.8160	19117	0.0478	9712.7487	19154	0.0481
8963.3905	17164	0.0333	8975.6298	17196.5	0.0346	9699.0047	19117.5	0.0483	9712.9368	19154.5	0.0479
8963.5807	17164.5	0.0351	8975.8196	17197	0.0361	9699.1926	19118	0.0479	9713.1252	19155	0.0481
8963.7673	17165	0.0335	8976.0063	17197.5	0.0346	9699.3812	19118.5	0.0483	9713.5019	19156	0.0481
8963.9570	17165.5	0.035	8976.1962	17198	0.0362	9699.5691	19119	0.0479	9713.6898	19156.5	0.0478
8964.1438	17166	0.0335	8976.3828	17198.5	0.0346	9699.7578	19119.5	0.0482	9713.8784	19157	0.0481
8964.3335	17166.5	0.035	8976.5729	17199	0.0363	9699.9456	19120	0.0479	9714.0664	19157.5	0.0478
8964.5204	17167	0.0336	8976.7594	17199.5	0.0345	9700.1344	19120.5	0.0483	9714.2550	19158	0.0482
8964.7101	17167.5	0.0349	8976.9495	17200	0.0364	9700.3221	19121	0.0478	9714.4429	19158.5	0.0477
8964.8970	17168	0.0336	8977.1360	17200.5	0.0345	9700.3222	19122	0.004	9714.6315	19159	0.0481
8965.0865	17168.5	0.0349	8977.3260	17201	0.0009	9700.5108	19121.5	0.0482	9714.8195	19159.5	0.0478
8965.2736	17169	0.0337	8977.5125	17201.5	0.0345	9700.6986	19122	0.0477	9715.0082	19160	0.0482
8965.4631	17169.5	0.0349	8977.7028	17202	0.0364	9700.8874	19122.5	0.0482	9715.1961	19160.5	0.0478
8965.6503	17170	0.0338	8977.8891	17202.5	0.0345	9701.0752	19123	0.0478	9715.1961	19160.5	0.0478
8965.8397	17170.5	0.0349	8978.0794	17203	0.0366	9701.2639	19123.5	0.0482	9715.3847	19161	0.0482
8966.0269	17171	0.0338	8978.2656	17203.5	0.0345	9701.4517	19124	0.0478	9715.5727	19161.5	0.0479
8966.2162	17171.5	0.0349	8978.4560	17204	0.0367	9701.6405	19124.5	0.0481	9715.7612	19162	0.0482
8966.4035	17172	0.0339	8978.6422	17204.5	0.0345	9701.8282	19125	0.0476			

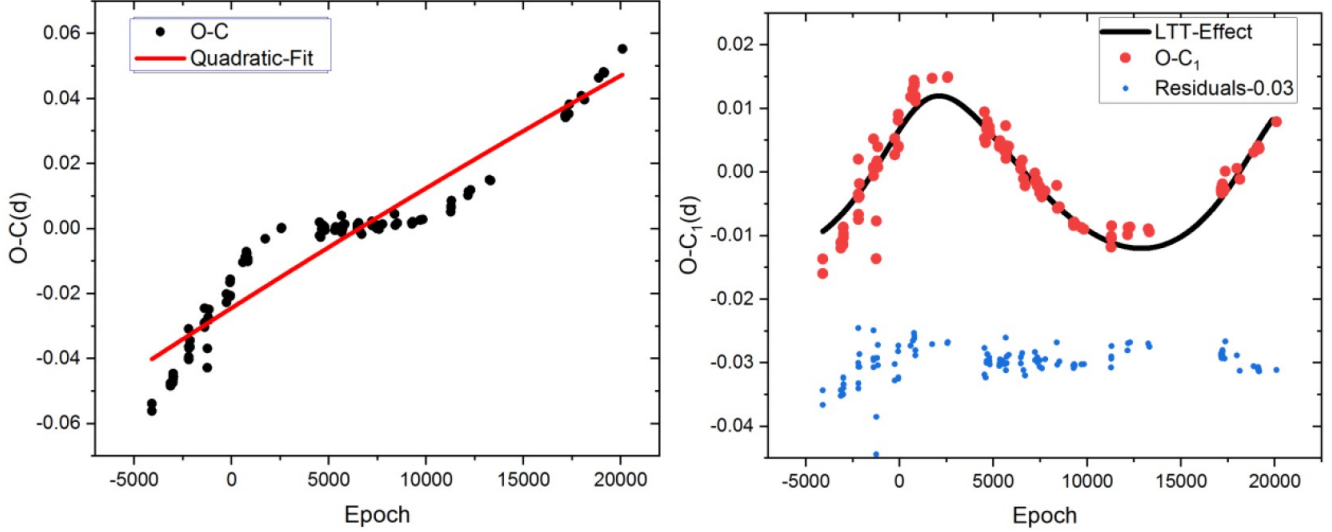


Figure 6. Left Panel: The O-C data points of the minima (black circle) and, the polynomial fit (red line). Right Panel: LTTE on the residuals of the polynomial fit; LTTE (black line), the O-C data points after subtracted polynomial fit (red circles), and the residuals of the LTTE effect fit (blue circles).

Table 4. Parameters of the third body.

Parameters of third body	Value
Eccentricity (e)	0.689 ± 0.005
The longitude of periastron passage (ω)	57.6 ± 1.8
Period (days)	7351.018
Amplitude (minutes)	17.28 ± 1.44
The time of periastron passage (T_0)	2460201
Projected semi-major axis $\times \sin i$	2.11 ± 0.17
Mass Function ($\text{MassFunction}(f_m)$)	0.023 ± 0.006
$M_3 \sin i (i = 90^\circ, M_\odot)$	0.498
$\sum (O - C)^2$	0.001

radial-velocity curve. We estimate that this figure is most likely due to systematic errors in background flux level readings in TESS photos and/or an underestimation of photometric aperture contamination by other stars in the image. So, we investigated the Applegate's effect as a plausible explanation for the cyclical fluctuations in the O-C curve. We calculated the observed relative change of the orbital period throughout one cycle of the binary using the previously obtained modulation period and the O-C amplitude computed from the orbit of the third body simulated in the previous section. $\frac{\Delta P}{P} = 2\pi \frac{(O-C)}{P_{\text{mod}}} = 1.025 \times 10^{-5}$ (Applegate 1992). The value of $\frac{\Delta P}{P}$ suggests that the Applegate effect can explain the cyclic changes in the O-C curve of minima.

This system shows unequal maxima that is known as the O'Connell effect (O'Connell 1951) due to the presence of the hot spots (Wilsey & Beaky 2009). So, this difference implies that the hemisphere of a component emits a different amount of radiation than the other hemisphere. These types of systems have active chromospheres because of the existence of large spots (Knote et al. 2022). Starspots can alter the depth of minima and have an obvious effect on the eclipse light curve (Han, Muirhead, & Swift 2019).

To investigate the effect of the spots on the light curve over both sectors of TESS observations, we calculated the difference between the two depths of the primary and secondary minima. We considered the relative fluxes in phases 0 and 0.5 for every complete individual light curve. The curves that resulted were displayed in Figure 7. YY CrB has the values of the DepthI - DepthII as large as about 10% of the variable light amplitude. And this is possible because

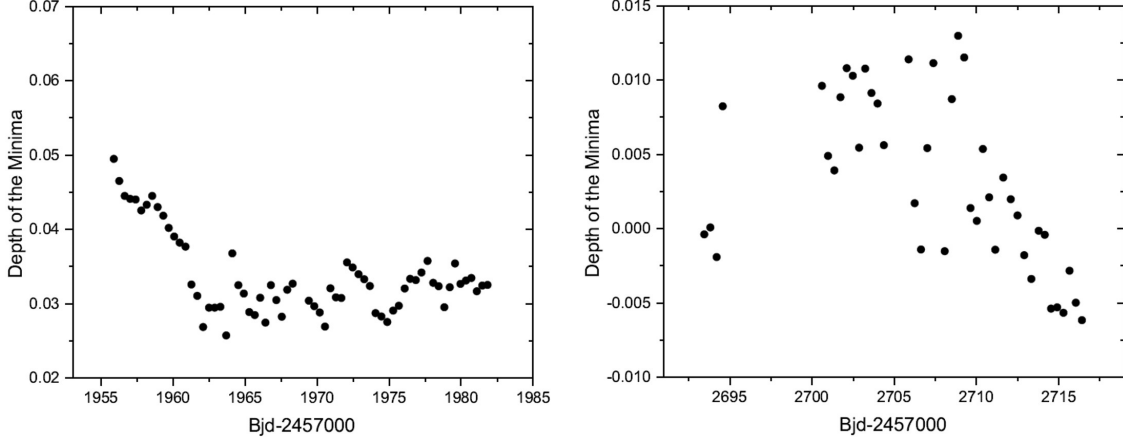


Figure 7. Right panel: the difference between the depths of Primary and Secondary minima over the 24th sector of TESS observations. Left panel: the difference between the depths of Primary and Secondary minima over the 51st sector of TESS observations.

of the migration and evolution of spots with time on the surface of two components that cause cyclic magnetic activity.

6. DISCUSSION AND CONCLUSION

Based on the estimated mass ratio, fill-out factor and inclination angle, YY CrB is an over-contact binary with an increased orbital period. Essam et al. (2010) calculated the decreased period rate $1.194 \times 10^{-6} \frac{\text{day}}{\text{year}}$. Yu, Xiang, & Xiao (2015) considered all of the minima time published until 2013 and calculated a secular period decrease with a rate of $6.727 \times 10^{-7} \frac{\text{day}}{\text{year}}$. In this study, the decreasing value of period rate $5.786 \times 10^{-8} \frac{\text{day}}{\text{year}}$ indicates that the rate of period changes has been decreased. And, when mass conservation is taken into account, the mass transfer from the Roche-lobe-filling primary component to the secondary component is $\dot{M} = 2.472 \times 10^{-8} M_{\odot} \text{yr}^{-1}$. When the stated results in Yu, Xiang, & Xiao (2015) are compared to the value of mass transfer in this study, it is clear that mass transfer has been decreased and the distance between two components is growing while the value of fill-out factor is decreasing (compare the values of fill-out factors in Table 1). And this target may evolve to shallow-contact binary via the thermal relaxation oscillation (TRO) model (Flannery (1976); Robertson & Eggleton (1977)) and ultimately reach a broken-contact phase (Lucy (1976)). The mass ratio of the components, which is related to the mass transfer, is the crucial parameter in the evolution of the close binary stars. Table 5 contains a list of contact binaries with low mass ratios < 0.25 . In order to explain the evolutionary status of the YY CrB system, we provide the mass-luminosity ($M - L$) diagram displayed in Figure 8. The Zero-Age Main Sequence (ZAMS) and the Terminal-Age Main Sequence (TAMS) are plotted along with the selected contact binaries with low mass ratios. It is obvious that the more massive primary components are around the ZAMS line, meaning they are not evolved or little evolved. Also, the less massive secondary components have evolved away from the main sequence stars and over-luminosity comparing the stars with the same mass in the main sequence. In addition, the orbital angular momentum of YY CrB has a value of 51.585 ± 0.067 . The $\log J_0 - \log M$ diagram shows the position of the system (Figure 9), and this diagram shows that YY CrB is in a contact binary systems region.

According to the study Yu, Xiang, & Xiao (2015) and the periodic changes in the residuals of the quadratic fit on the O-C curve, the potential of excitability of the third body was investigated. The light-time function fitting revealed the existence of a body with the value of $0.498 M_{\odot}$. This number equates to 0.016 of total brightness, which differs from the value of l_3 determined in section 3. We explored the Applegate effect as a possible explanation for the fluctuation in the O-C curve because there is no exact radial-velocity curve.

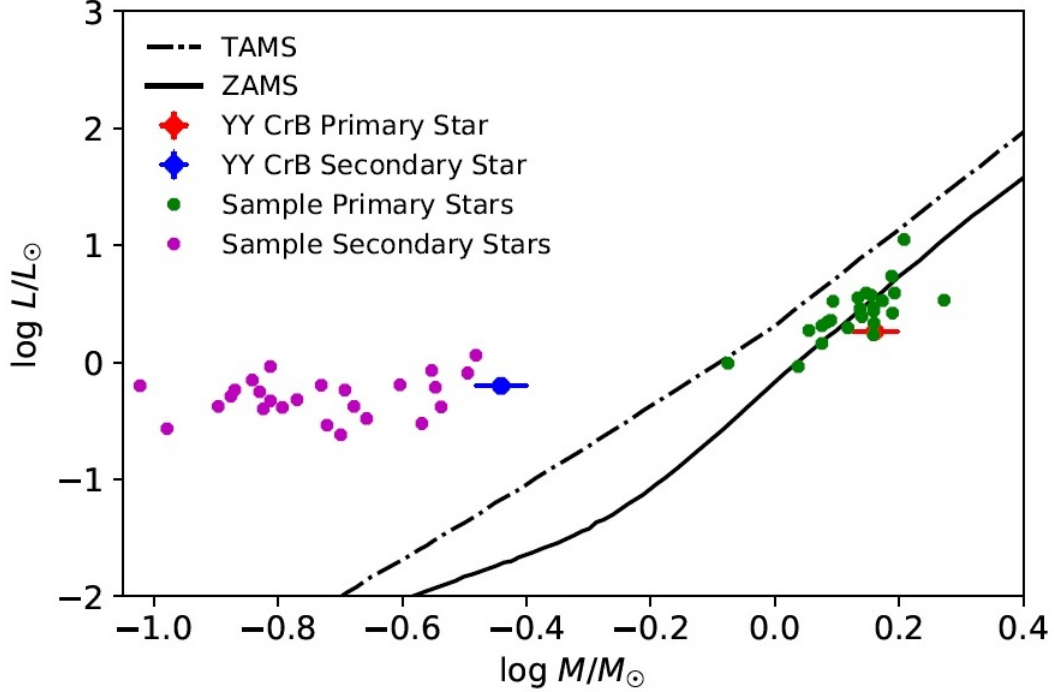


Figure 8. $M - L$ diagram of selected contact binaries with low mass ratio. The primary and secondary components of YY CrB are plotted in red and blue colors, respectively.

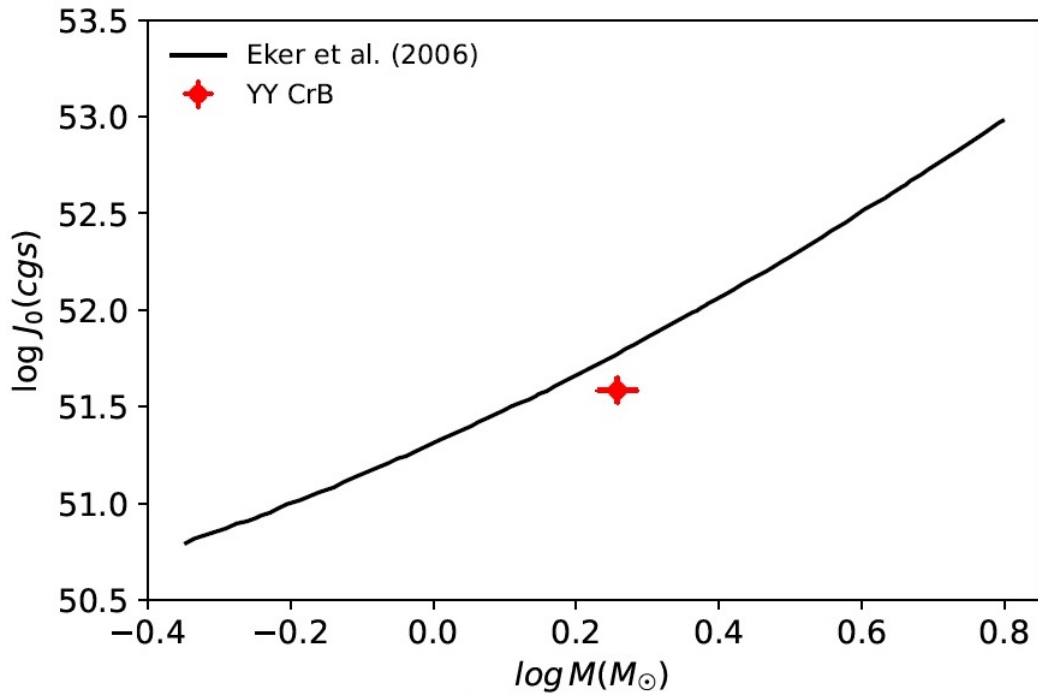


Figure 9. The location of YY CrB on the $\log J_0 - \log M$ diagram. The quadratic line is based on a study by [Eker et al. \(2006\)](#).

Table 5. Absolute parameters for low mass ratio contact binaries.

System	q	$M_1(M_\odot)$	$M_2(M_\odot)$	$R_1(R_\odot)$	$R_2(R_\odot)$	$L_1(L_\odot)$	$L_2(L_\odot)$	Reference
V429 Cam	0.206	1.36(12)	0.28(3)	1.55(3)	0.78(2)	3.56(9)	0.85(2)	Li et al. (2021)
V830 Cep	0.23	0.84(5)	0.19(1)	0.91(1)	0.47(1)	0.98(1)	0.29(1)	Li et al. (2021)
FP Boo	0.096	1.614(52)	0.154(21)	2.310(25)	0.774(8)	11.193(99)	0.920(13)	Gazeas et al. (2006)
DN Boo	0.103	1.428(39)	0.148(6)	1.710(67)	0.670(110)	3.750(280)	0.560(170)	Şenavci et al. (2008)
FG Hya	0.112	1.444(25)	0.161(7)	1.405(9)	0.591(8)	2.158(86)	0.412(17)	Qian & Yang (2005)
CK Boo	0.0108	1.442(14)	0.154(2)	1.453(3)	0.577(10)	2.74(1)	0.47(2)	Kalci & Derman (2005)
GR Vir	0.122	1.37(16)	0.17(6)	1.42(7)	0.61(4)	2.87(28)	0.48(6)	Qian & Yang (2004)
CSS J234807.2+193717	0.176	1.19(4)	0.21(3)	1.36 (2)	0.66 (1)	1.45(24)	0.42(5)	Christopoulou et al. (2022)
J170307	0.092	1.134(253)	0.105(24)	1.204(120)	0.436(48)	1.874(572)	0.271(72)	Liu et al. (2023)
J1641000	0.095	1.402(287)	0.133(28)	1.580(144)	0.577(58)	3.912(1.109)	0.512(142)	Liu et al. (2023)
J223837	0.093	1.541(306)	0.144(30)	1.784(159)	0.646(64)	5.463(1.534)	0.704(192)	Liu et al. (2023)
CSS J222607.8+062107	0.221	1.49(3)	0.33(13)	1.51(5)	0.81(2)	3.35(65)	1.15(24)	Sun et al. (2020)
CSS J012559.7+203404	0.231	1.38(3)	0.32(12)	1.42(4)	0.77(2)	2.46(56)	0.81(18)	Sun et al. (2020)
CSS J153855.6+042903	0.187	1.44(5)	0.27(12)	1.37(4)	0.66(2)	2.94(96)	0.30(10)	Sun et al. (2020)
CSS J141923.2–013522	0.168	1.31(5)	0.22(11)	1.23(4)	0.57(2)	1.97(68)	0.33(11)	Sun et al. (2020)
CSS J130111.2–132012	0.108	1.38(3)	0.15(12)	1.49(5)	0.61(2)	2.49(57)	0.40(9)	Sun et al. (2020)
CSS J165813.7+390911	0.183	1.09(3)	0.20(9)	1.05(3)	0.49(1)	0.92(24)	0.24(6)	Sun et al. (2020)
V870 Ara	0.082	1.546(54)	0.127(37)	1.64(6)	0.63(5)	2.64(17)	0.42(6)	Poro et al. (2021)
TYC 6995-813-1	0.111	1.23(1)	0.135(1)	1.46(1)	0.60(1)	2.293(4)	0.58(2)	Wadhwa et al. (2021)
NSVS 13602901	0.171	1.19(2)	0.203(10)	1.69(1)	0.79(1)	2.05(4)	0.58(2)	Wadhwa et al. (2021)
NSVS 5029961	0.151	1.872(468)	0.284(72)	1.573(119)	0.680(53)	3.403(14)	0.610(26)	Zheng et al. (2021)
CSS J022914.4+044340	0.201	1.44(25)	0.29(5)	1.26(8)	0.65(4)	1.718(191)	0.416(50)	Liu & Li (2021)
HV Aqr	0.15	1.240(28)	0.186(17)	1.456(12)	0.601(5)	3.326(213)	0.638(44)	Gazeas et al. (2021)
ZZ PsA	0.078	1.213(8)	0.095(1)	1.422(4)	0.559(4)	2.20(4)	0.63(4)	Wadhwa et al. (2021)
NSVS 1926064	0.160	1.558(38)	0.249(6)	1.605(13)	0.755(42)	3.91(28)	0.641(33)	Kjurkchieva et al. (2020)

YY CrB is a contact binary with a mass ratio less than 0.3, so considering Hut's criteria (Hut 1980) to investigate the stability is necessary. We used Equation (15) to calculate the ratio of the spin angular momentum to the orbital angular momentum (Yang & Qian 2015).

$$\frac{J_s}{J_o} = \frac{q+1}{q} [(k_1 r_1)^2 + (k_2 r_2)^2 q] \quad (15)$$

where r_1 and r_2 are the relative radii for the primary and secondary components and $k^2_{1,2} = 0.06$ (Li & Zhang 2006), are the dimensionless gyration radii. The calculated value of $\frac{J_s}{J_o} = 0.087$, which is less than the threshold value therefore this system is stable. This target shows a period increase which is attributed to mass transfer. According to the existing data and the analyses done in this study, the existence of a third body is unlikely for this system, and detailed spectroscopic and photometric observations over a longer length of time are required for the definitive determination.

ACKNOWLEDGEMENTS

This manuscript has made use of data from the TESS mission. Funding for the TESS mission is provided by the NASA Science Mission Directorate. This research has made use of the SIMBAD and VIZIER databases, operated at CDS, Strasbourg, France. The time of minima data from the Variable Star Observers League in Japan (VSOLJ) websites proved invaluable to the assessment of potential period changes experienced by this variable star. The authors would like to thank Marco Brentel for his help. We are grateful to Ehsan Paki from the BSN project (<https://bsnp.info/>) for providing Figure 4 of this manuscript, which also shows the color-temperature scale.

ORCID IDS

Somayeh Soomandar: 0000-0002-9520-9573
Atila Poro: 0000-0002-0196-9732

APPENDIX

A. AVAILABLE MINIMA TIMES

The appendix table displays the minima times along with their error in the first column, the epochs in the third column, the O-C values in the fourth column, and the references in the final column.

Table 1. Available mid-eclipse times of YY CrB system. ons. All minimum have been reduced to 2450000

Min.(BJD_{TDB})	Epoch	O-C	Reference	Min.(BJD_{TDB})	Epoch	O-C	Reference
955.8695(12)	-4101	-0.0562	Pribulla et al. (2001)	4308.3899(2)	4802	-0.0005	Parimucha et al. (2009)
955.8718(6)	-4101	-0.0539	Rucinski, et al. (2000)	4564.2595	5481.5	0.0003	Nagai (2009)
1318.4993	-3138	-0.04847	Essam et al. (2010)	4604.36215(1)	5588	-0.0001	Yilmaz et al. (2009)
1318.5001	-3138	-0.0475	Essam et al. (2010)	4605.4917(2)	5591	-0.0002	Yilmaz et al. (2009)
1361.4275(3)	-3024	-0.0475	Keskin et al. (2000)	4628.4657(2)	5652	0.0039	Parimucha et al. (2009)
1361.4275(2)	-3024	-0.0474	Keskin et al. (2000)	4632.4144(3)	5662.5	-0.0012	Parimucha et al. (2009)
1368.3965(4)	-3005.5	-0.0447	Keskin et al. (2000)	4648.4191(30)	5706	0.0000	Parimucha et al. (2009)
1368.3966(4)	-3005.5	-0.0446	Keskin et al. (2000)	4648.4201(10)	5705	0.0009	Hubscher et al. (2009)
1370.4659(6)	-3000	-0.0463	Keskin et al. (2000)	4688.3352(3)	5811	0.0013	Yilmaz et al. (2009)
1372.3494(3)	-2995	-0.0457	Keskin et al. (2000)	4931.4009(1)	6456.5	0.0011	Hubscher et al. (2011)
1668.3359	-2209	-0.0309	Essam et al. (2010)	4931.5883(1)	6457	0.0001	Hubscher et al. (2011)
1669.4602	-2206	-0.0363	Essam et al. (2010)	4958.5136(20)	6528.5	0.0018	Hubscher et al. (2011)
1670.3976	-2203.5	-0.0403	Essam et al. (2010)	4983.7401(3)	6595.5	-0.0009	Diethelm (2009)
1670.3984	-2203.5	-0.0395	Essam et al. (2010)	5017.44086(3)	6685	-0.0017	Parimucha et al. (2009)
1674.3548	-2193	-0.0369	Karska & Maciejewski (2003)	5213.6297(3)	7206	0.0022	Parimucha et al. (2011)
1692.4299	-2144	-0.0365	Essam et al. (2010)	5219.6532(1)	7222	0.0009	Parimucha et al. (2011)
1692.4319	-2145	-0.0345	Essam et al. (2010)	5261.8279(1)	7334	0.0014	Dvorak (2011)
1975.6050	-1392	-0.0304	Pribulla, et al. (2003)	5264.4630(3)	7341	0.0006	Parimucha et al. (2011)
1975.6061(1)	-1392	-0.0293	Pribulla et al. (2001)	5311.3444(2)	7465.5	0.001	Parimucha et al. (2011)
1975.6064(1)	-1393	-0.0290	Pribulla et al. (2001)	5311.5317(2)	7466	0.000	Parimucha et al. (2011)
1975.6108(7)	-1392	-0.0246	Pribulla & Vanko (2002)	5351.4463(1)	7572	-0.0002	Hubscher, et al. (2012)
2029.4398(7)	-1250	-0.0426	Pribulla & Vanko (2002)	5354.4587(2)	7580	-0.0002	Parimucha et al. (2011)
2031.5168(7)	-1244.5	-0.0369	Pribulla & Vanko (2002))	5420.3573(3)	7755	0.0137	Parimucha et al. (2011))
2045.4589	-1207.5	-0.0273	Essam et al. (2010)	5652.8828(30)	8372.5	0.0045	Diethelm (2011)
2060.3320	-1167	-0.0281	Essam et al. (2010)	5665.4931(3)	8406	0.0088	Parimucha et al. (2013)
2060.3352	-1167	-0.0249	Essam et al. (2010)	5705.4093(23)	8512	0.0016	Hubscher, et al. (2012)
2400.1804(2)	-265.5	-0.0202	Pribulla et al. (2002)	6011.5475(2)	9325	0.0051	Parimucha et al. (2013)
2400.3660	-264	-0.0227	Karska & Maciejewski (2003)	55987.6371(2)	9261.5	0.0018	Parimucha et al. (2013)
2469.4699(4)	-81.5	-0.017	Demircan et al. (2003)	5987.6371(2)	9261.5	0.0018	Parimucha et al. (2013)
2472.2898(2)	-74	-0.0209	Petropoulou et al. (2015)	5992.5319(2)	9274.5	0.0014	Parimucha et al. (2013)
2473.4197(2)	-71	-0.0206	Petropoulou et al. (2015)	6005.5237(2)	9309	0.0021	Parimucha et al. (2013)
2473.4247(4)	-71	-0.0156	Demircan et al. (2003)	6005.5237(2)	9309	0.0021	Parimucha et al. (2013)
2500.1757	0	0.000	Kreiner (2004)	6149.3679(2)	9691	0.0026	Parimucha et al. (2013)
2719.3200	582	-0.0104	Nagai (2004)	2456199.26169(2)	9823.5	0.0028	Parimucha et al. (2013)
2764.5082(23)	702	-0.0088	Hubscher et al. (2005)	6742.4439(14)	11266	0.00513	Hubscher & Lehmann (2015)
2786.3500(2)	761	-0.0071	Ak & Filiz (2003)	6749.4115(5)	11284.5	0.0066	Hubscher & Lehmann (2015)
2793.5038(2)	779	-0.0079	Ak & Filiz (2003)	6011.5483(2)	9325	0.0018	Parimucha et al. (2013)
7074.9466(1)	12149	0.010	Nelson (2016)	6754.4970(35)	11298	0.0086	Hubscher & Lehmann (2015)
2793.5042(21)	779	-0.0075	Hubscher et al. (2005)	7074.9466(1)	12149	0.010	Nelson (2016)
2814.4011(1)	834.5	-0.0093	Selam et al. (2003)	7084.1734	12173.5	0.0114	Nagai (2016)
3151.0470	1728.5	-0.0032	Nagai (2005)	7123.5238(28)	12278	-0.011	Hubscher (2017))
3458.8835(2)	2546	0.000	Dvorak (2006)	6749.6002(8)	11285	0.0068	Hubscher & Lehmann (2015)
3466.41483(1)	2566	0.000	Pribulla et al. (2005)	7513.0723	13312.5	0.0147	Nagai (2017)
4201.4509(16)	4518	0.0020	Hubscher (2007)	7489.5378(18)	13250	0.015	Hubscher (2017)
4201.6350(17)	4518.5	-0.0022	Hubscher (2007)	9024.3943	17326	0.0353	Nagai (2021)
4245.5055(9)	4635	-0.0003	Brát, et al. (2007)	9037.3884	17360.5	0.0382	Nagai (2021)
4224.4161(2)	4579	-0.0028	Parimucha et al. (2009)	9269.5368(10)	17977	0.0408	Paschke (2021)
4300.4828(1)	4781	0.0000	Parimucha et al. (2009)	9328.4664(7)	18133.5	0.0398	Lienhard (2022)
4500.6209(3)	5312.5	-0.0006	Parimucha et al. (2009)	9605.99382(1)	18870.5	0.0464	Nelson & Alton (2022)
4504.5751(8)	5323	-0.0002	Parimucha et al. (2009)	10064.4578(30)	20088	0.0553	Paschke (2023)
14513.6131(6)	5347	0.0005	Parimucha et al. (2009)				
14560.1297	5470.5	0.0126	Nagai (2009)				

REFERENCES

- Ak H., Filiz N., 2003, Photoelectric Minimum Times of Some Eclipsing Binary Stars, IBVS, 5462, 1
- Applegate J. H., 1992, A Mechanism for Orbital Period Modulation in Close Binaries, ApJ, 385, 621. doi:10.1086/170967
- Balaji B., Croll B., Levine A. M., Rappaport S., 2015, Tracking the stellar longitudes of starspots in short-period Kepler binaries, MNRAS, 448, 429. doi:10.1093/mnras/stv031
- Brát L., Zejda M., Svoboda P., 2007, B.R.N.O. Contributions 34, OEJV, 0074, 1
- Castelli F., Kurucz R. L., 2004, Is missing Fe I opacity in stellar atmospheres a significant problem?, A&A, 419, 725. doi:10.1051/0004-6361:20040079
- Conroy K. E., Kochoska A., Hey D., Pablo H., Hambleton K. M., Jones D., Giammarco J., et al., 2020, Physics of Eclipsing Binaries. V. General Framework for Solving the Inverse Problem, ApJS, 250, 34. doi:10.3847/1538-4365/abb4e2
- Christopoulou P.-E., Lalounta E., Papageorgiou A., Ferreira Lopes C. E., Catelan M., Drake A. J., 2022, New low mass ratio contact binaries in the Catalina Sky Survey, MNRAS, 512, 1244. doi:10.1093/mnras/stac534
- Demircan O., Erdem A., Ozdemir S., Cicek C., Bulut I., Soydugan F., Soydugan E., et al., 2003, The First Eclipsing Binary Observations at the Ulupinar Astrophysics Observatory, IBVS, 5364, 1
- Diethelm R., 2009, Timings of Minima of Eclipsing Binaries, IBVS, 5894, 1
- Diethelm R., 2011, Timings of Minima of Eclipsing Binaries, IBVS, 5960, 1
- Dvorak S. W., 2006, Times of Minima for Neglected Eclipsing Binaries in 2005, IBVS, 5677, 1
- Dvorak S. W., 2011, Times of Minima for Eclipsing Binaries 2010, IBVS, 5974, 1
- Eker Z., Demircan O., Bilir S., Karataş Y., 2006, Dynamical evolution of active detached binaries on the log \dot{J} -logM diagram and contact binary formation, MNRAS, 373, 1483. doi:10.1111/j.1365-2966.2006.11073.x
- ESA, 1997, The HIPPARCOS and TYCHO catalogues. Astrometric and photometric star catalogues derived from the ESA HIPPARCOS Space Astrometry Mission, ESASP, 1200
- Essam A., Saad S. M., Nouh M. I., Dumitrescu A., El-Khateeb M. M., Haroon A., 2010, Photometric and spectroscopic analysis of YY CrB, NewA, 15, 227. doi:10.1016/j.newast.2009.07.006
- Flannery B. P., 1976, A Cyclic Thermal Instability in Contact Binary Stars, ApJ, 205, 217. doi:10.1086/154266
- Flower P. J., 1996, Transformations from Theoretical Hertzsprung-Russell Diagrams to Color-Magnitude Diagrams: Effective Temperatures, B-V Colors, and Bolometric Corrections, ApJ, 469, 355. doi:10.1086/177785
- Gazeas K. D., Baran A., Niarchos P., Zola S., Kreiner J. M., Ogloza W., Rucinski S. M., et al., 2005, Physical Parameters of Components in Close Binary Systems: IV, AcA, 55, 123
- Gazeas K. D., Niarchos P. G., Zola S., Kreiner J. M., Rucinski S. M., 2006, Physical Parameters of Components in Close Binary Systems: VI AcA, 56, 127. doi:10.48550/arXiv.0903.1364
- Green G. M., Schlafly E., Zucker C., Speagle J. S., Finkbeiner D., 2019, A 3D Dust Map Based on Gaia, Pan-STARRS 1, and 2MASS, ApJ, 887, 93. doi:10.3847/1538-4357/ab5362
- Han E., Muirhead P. S., Swift J. J., 2019, Magnetic Inflation and Stellar Mass. IV. Four Low-mass Kepler Eclipsing Binaries Consistent with Non-magnetic Stellar Evolutionary Models, AJ, 158, 111. doi:10.3847/1538-3881/ab2ed7
- Hubscher J., Lehmann P. B., 2015, BAV-Results of observations - Photoelectric Minima of Selected Eclipsing Binaries and Maxima of Pulsating Stars, IBVS, 6149, 1
- Hubscher J., Paschke A., Walter F., 2005, Photoelectric Minima of Selected Eclipsing Binaries and Maxima of Pulsating Stars, IBVS, 5657, 1
- Hubscher J., Paschke A., Walter F., 2006, Photoelectric Minima of Selected Eclipsing Binaries and Maxima of Pulsating Stars, IBVS, 5731, 1
- Hubscher J., Steinbach H.-M., Walter F., 2009, BAV-Results of observations - Photoelectric Minima of Selected Eclipsing Binaries and Maxima of Pulsating Stars, IBVS, 5874, 1
- Hubscher J., Lehmann P. B., Monninger G., Steinbach H.-M., Walter F., 2011, VizieR Online Data Catalog: Minima and maxima of 452 variables, yCatp, 0185, J/other/IBVS/5918
- Hubscher J., Lehmann P. B., Walter F., 2012, BAV-Results of observations - Photoelectric Minima of Selected Eclipsing Binaries and Maxima of Pulsating Stars, IBVS, 6010, 1
- Hubscher J., 2007, Photoelectric Minima of Selected Eclipsing Binaries and Maxima of Pulsating Stars, IBVS, 5802, 1

- Hubscher J., 2017, BAV-Results of observations - Photoelectric Minima of Selected Eclipsing Binaries and Maxima of Pulsating Stars, IBVS, 6196, 1.
doi:10.22444/IBVS.6196
- Hut P., 1980, Stability of tidal equilibrium, A&A, 92, 167
- Irwin J. B., 1952, The Determination of a Light-Time Orbit, ApJ, 116, 211. doi:10.1086/145604
- Jenkins J. M., Twicken J. D., McCauliff S., Campbell J., Sanderfer D., Lung D., Mansouri-Samani M., et al., 2016, The TESS science processing operations center, SPIE, 9913, 99133E. doi:10.1117/12.2233418
- Jenkins J. M., 2015, Overview of the TESS Science Pipeline, ESS
- Kalci R., Derman E., 2005, CK Bootis: a W UMa system with a small mass ratio, AN, 326, 342.
doi:10.1002/asna.200510361
- Karska A., Maciejewski G., 2003, CCD Times of Minima of Some Eclipsing Binaries in 2002, IBVS, 5380, 1
- Keskin V., Yasarsoy B., Sipahi E., 2000, Times of Minima of Some Eclipsing Binaries, IBVS, 4855, 1
- Knote M. F., Caballero-Nieves S. M., Gokhale V., Johnston K. B., Perlman E. S., 2022, Characteristics of Kepler Eclipsing Binaries Displaying a Significant O'Connell Effect, ApJS, 262, 10. doi:10.3847/1538-4365/ac770f
- Kreiner J. M., 2004, Up-to-Date Linear Elements of Eclipsing Binaries, AcA, 54, 207
- Lenz P., Breger M., 2005, Period04 User Guide, CoAst, 146, 53. doi:10.1553/cia146s53
- Li L., Zhang F., 2006, The dynamical stability of W Ursae Majoris-type systems, MNRAS, 369, 2001.
doi:10.1111/j.1365-2966.2006.10462.x
- Li K., Xia Q.-Q., Kim C.-H., Gao X., Hu S.-M., Guo D.-F., Gao D.-Y., et al., 2021, Photometric Study and Absolute Parameter Estimation of Six Totally Eclipsing Contact Binaries, AJ, 162, 13. doi:10.3847/1538-3881/abfc53
- Lightkurve Collaboration, Cardoso J. V. de M., Hedges C., Gully-Santiago M., Saunders N., Cody A. M., Barclay T., et al., 2018, Lightkurve: Kepler and TESS time series analysis in Python, ascl.soft. ascl:1812.013
- Lucy L. B., 1967, Gravity-Darkening for Stars with Convective Envelopes, ZA, 65, 89
- Lucy L. B., 1976, W Ursae Majoris systems with marginal contact, ApJ, 205, 208. doi:10.1086/154265
- Nagai, K., 2004, Visual and CCD minima of eclipsing binaries during 2003, Variable Star Bulletin, No.42, 1
- Nagai, K., 2005, Visual and CCD minima of eclipsing binaries during 2004, Variable Star Bulletin, No. 43, 1
- Nagai, K., 2009, Visual and CCD minima of eclipsing binaries during 2008, Variable Star Bull. No. 48, 1
- Nagai, K., 2016, Visual,CCD and DSLR minima of eclipsing binaries during 2015, Variable Star Bulletin, No. 61, 1
- Nagai, K., 2017, Visual,CCD and DSLR minima of eclipsing binaries during 2016, Variable Star Bulletin, No. 63, 1
- Nagai, K., 2021, Visual,CCD and DSLR minima of eclipsing binaries during 2020, Variable Star Bulletin, No. 69, 1
- Nelson R. H., 2016, CCD Minima for Selected Eclipsing Binaries in 2015, IBVS, 6164, 1
- O'Connell D. J. K., 1951, The so-called periastron effect in close eclipsing binaries ; New variable stars (fifth list), PRCO, 2, 85
- Parimucha S., Dubovsky P., Baludansky D., Pribulla T., Hambalek L., Vanko M., Ogloza W., 2009, Minima Times of Selected Eclipsing Binaries, IBVS, 5898, 1
- Parimucha S., Dubovsky P., Vanko M., Pribulla T., Kudzej I., Barsa R., 2011, Minima Times of Selected Eclipsing Binaries, IBVS, 5980, 1
- Parimucha S., Dubovsky P., Vanko M., 2013, Minima Times of Selected Eclipsing Binaries, IBVS, 6044, 1
- Patra K. C., Winn J. N., Holman M. J., Yu L., Deming D., Dai F., 2017, The Apparently Decaying Orbit of WASP-12b, AJ, 154, 4. doi:10.3847/1538-3881/aa6d75
- Petropoulou M., Gazeas K., Tzouganatos L., Karampotsiou E., 2015, 110 minima timings of eclipsing binaries, IBVS, 6153, 1
- Pogson N., 1856, Magnitudes of Thirty-six of the Minor Planets for the first day of each month of the year 1857, MNRAS, 17, 12. doi:10.1093/mnras/17.1.12
- Poro A., Sarabi S., Zamanpour S., Fotouhi S., Davoudi F., Khakpash S., Salehian S. R., et al., 2022, Investigation of the orbital period and mass relations for W UMa-type contact systems, MNRAS, 510, 5315.
doi:10.1093/mnras/stab3775
- Poro A., Paki E., Blackford M. G., Davoudi F., Aladag Y., Zamanpour S., Sarabi S., et al., 2022, The Photometric Study of Six W UMa Systems and Investigation of the Mass-Radius Relations for Contact Binary Stars, PASP, 134, 064201. doi:10.1088/1538-3873/ac71cd
- Prša A., Conroy K. E., Horvat M., Pablo H., Kochoska A., Bloemen S., Giammarco J., et al., 2016, Physics Of Eclipsing Binaries. II. Toward the Increased Model Fidelity, ApJS, 227, 29. doi:10.3847/1538-4365/227/2/29
- Prša A., Zwitter T., 2005, A Computational Guide to Physics of Eclipsing Binaries. I. Demonstrations and Perspectives, ApJ, 628, 426. doi:10.1086/430591
- Pribulla T., Vanko M., 2002, Photoelectric photometry of eclipsing contact binaries: U Peg, YY CrB, OU Ser and EQ Tau, CoSka, 32, 79

- Pribulla T., Vanko M., Parimucha S., Chochol D., 2001, New Photoelectric Minima and Updated Ephemerides of Selected Eclipsing Binaries, IBVS, 5056, 1
- Pribulla T., Vanko M., Parimucha S., Chochol D., 2002, IBVS, 5341, 1
- Pribulla T., Kreiner J. M., Tremko J., 2003, New Photoelectric and CCD Minima and Updated Ephemerides of Selected Eclipsing Binaries, CoSka, 33, 38
- Pribulla T., Baludansky D., Chochol D., Chrastina M., Parimucha S., Petrik K., Szasz G., et al., 2005, New Minima of Selected Eclipsing Close Binaries, IBVS, 5668, 1
- Qian S.-B., Yang Y.-G., 2004, GR Virginis: A Deep Overcontact Binary, AJ, 128, 2430. doi:10.1086/425051
- Qian S., Yang Y., 2005, Improved astrophysical parameters for the overcontact binary FG Hydræ, MNRAS, 356, 765. doi:10.1111/j.1365-2966.2004.08497.x
- Robertson J. A., Eggleton P. P., 1977, The evolution of W Ursae Majoris systems, MNRAS, 179, 359. doi:10.1093/mnras/179.3.359
- Ruciński S. M., 1969, The Proximity Effects in Close Binary Systems. II. The Bolometric Reflection Effect for Stars with Deep Convective Envelopes, AcA, 19, 245
- Rucinski S. M., Lu W., Mochnacki S. W., 2000, Radial Velocity Studies of Close Binary Stars. III, AJ, 120, 1133. doi:10.1086/301458
- Selam S. O., Albayrak B., Senavci H. V., Tanrıverdi T., Elmaslı A., Kara A., Aksu O., et al., 2003, Photoelectric Minima of Some Eclipsing Binary Stars, IBVS, 5471, 1
- Senavci H. V., Nelson R. H., Özavcı İ., Selam S. O., Albayrak B., 2008, 2008NewA...13..468S, NewA, 13, 468. doi:10.1016/j.newast.2008.01.001
- Sterken, C. 2005, The Light-Time Effect in Astrophysics: Causes and cures of the O-C diagram, 335, 3
- Soomandar S., Abedi A., 2020, First study of a low-amplitude eclipsing binary KIC11496078, NewA, 80, 101394. doi:10.1016/j.newast.2020.101394
- Sterken C., 2005, Binary Pulsars, General Relativity and Light-Time Effects, ASPC, 335, 215
- Torres G., 2010, On the Use of Empirical Bolometric Corrections for Stars, AJ, 140, 1158. doi:10.1088/0004-6256/140/5/1158
- Tran K., Levine A., Rappaport S., Borkovits T., Csizmadia S., Kalomeni B., 2013, The Anticorrelated Nature of the Primary and Secondary Eclipse Timing Variations for the Kepler Contact Binaries, ApJ, 774, 81. doi:10.1088/0004-637X/774/1/81
- Vaňko M., Parimucha Š., Pribulla T., Chochol D., 2004, New Parameters of the Contact Binary Systems YY CRB and EQ Tau, BaltA, 13, 151
- Wilsey N. J., Beaky M. M., 2009, Revisiting the O'Connell Effect in Eclipsing Binary Systems, SASS, 28, 107
- Yang Y.-G., Qian S.-B., 2015, Deep, Low Mass Ratio Overcontact Binary Systems. XIV. A Statistical Analysis of 46 Sample Binaries, AJ, 150, 69. doi:10.1088/0004-6256/150/3/69
- Yilmaz M., Basturk O., Alan N., Senavci H. V., Tanrıverdi T., Kılıçoglu T., Caliskan S., et al., 2009, New Times of Minima of Some Eclipsing Binary Stars and Maxima of Pulsating Stars, IBVS, 5887, 1
- Yu Y.-X., Xiang F.-Y., Xiao T.-Y., 2015, Orbital period changes of YY Coronæ Borealis, PASJ, 67, 42. doi:10.1093/pasj/psv014
- Liu X.-Y., Li K., Michel R., Gao X., Gao X., Liu F., Yin S.-P., et al., 2023, The study of 11 contact binaries with mass ratios less than 0.1, MNRAS, 519, 5760. doi:10.1093/mnras/stad026
- Sun W., Chen X., Deng L., de Grijs R., 2020, Physical Parameters of Late-type Contact Binaries in the Northern Catalina Sky Survey, ApJS, 247, 50. doi:10.3847/1538-4365/ab7894
- Poro A., Blackford M. G., Davoudi F., Mohandes A., Madani M., Rezaei S., Bozorgzadeh E., 2021, The New Ephemeris and Light Curve Analysis of V870 Ara by the Ground-Based and TESS Data, OASt, 30, 37. doi:10.1515/astro-2021-0004
- Wadhwa S. S., Tothill N. F. H., DeHorta A. Y., Filipović M., 2021, Photometric analysis of two extreme low mass ratio contact binary systems, RAA, 21, 235. doi:10.1088/1674-4527/21/9/235
- Zheng S.-Y., Li K., Xia Q.-Q., 2021, The first photometric and spectroscopic analysis of the extremely low mass-ratio contact binary NSVS 5029961, MNRAS, 506, 4251. doi:10.1093/mnras/stab1829
- Liu L., Li X.-Z., 2021, The deep and low-mass-ratio contact binary CSS J022914.4+044340 with a luminous additional companion, RAA, 21, 180. doi:10.1088/1674-4527/21/7/180
- Gazeas K., Zola S., Liakos A., Zakrzewski B., Rucinski S. M., Kreiner J. M., Ogloza W., et al., 2021, Physical parameters of close binary systems: VIII, MNRAS, 501, 2897. doi:10.1093/mnras/staa3753
- Kjurkchieva D. P., Popov V. A., Petrov N. I., 2020, Global parameters of the totally-eclipsing W UMa stars NSVS 6673994, NSVS 4316778, PP Lac and NSVS 1926064, NewA, 77, 101352. doi:10.1016/j.newast.2019.101352

- Wadhwa S. S., De Horta A., Filipović M. D., Tothill N. F. H., Arbutina B., Petrović J., Djurašević G., 2021, ZZ Piscis Austrinus (ZZ PsA): a bright red nova progenitor and the instability mass ratio of contact binary stars, MNRAS, 501, 229.
doi:10.1093/mnras/staa3637
- Paschke, A., 2021, A LIST OF MINIMA AND MAXIMA TIMINGS, BAV Journal. No. 55, 1
- Paschke, A., 2023, A LIST OF MINIMA AND MAXIMA TIMINGS BAV Journal. No. 79, 1

- Lienhard, P., 2022, BAV-Results of observations - Photoelectric Minima/Maxima of Selected Eclipsing Binaries and Maxima/Minima of Pulsating Stars, BAV Journal. No. 60, 1
- Nelson R. H., Alton K. B., 2022, CCD Minima for Selected Eclipsing Binaries in 2022, OEJV, 234, 1.
doi:10.5817/OEJV2022-0234